RESEARCH ARTICLE

MOLECULAR DOCKING STUDY, SYNTHESIS AND INVITRO EVALUATION OF ANTITUMOR ACTIVITY OF NOVEL NAPHTHYLIDENE BASE OF BENZOIC ACID DERIVATIVES

J.Nelson Samuel Jebastin[1]*, T. Ramesh Kumar[1] and D.Evangelin[2]

[1]Department of Zoology, Annamalai University, Annamalai Nagar-608 002, India.

[2]Department of Information Technology, Sri Vidya Engineering College, Virudhunagar, India

Email: arthik03@yahoo.com

Abstract: Cancer therapies targeted developing cell cycle-based mechanism that emulates the body's natural process in order to stop the growth of cancer cells. This approach can limit the damage to normal cells and the accompanying side effects caused by conventional chemotherapeutic agents. Inhibition of histone deacetylase (HDAC) enzymes is emerging as an innovative and effective approach for the treatment of cancer. Nineteen compounds of naphthylidene base of benzoic acid derivatives were designed and tested in silico for their interaction with histone deacetylase (HDAC8) enzyme. 19 ligands docked with Histone deacetylase 8 Human HDAC8 (PDB ID: 1T69) using Glide program (Version 5.0, Schrodinger, LLC, New York, 2008) and designed, synthesized and evaluated for their ability to inhibit cell proliferation in cancer cell lines. Based on the docking score 4-((2-hydroxynaphthalen-1-yl)methyleneamino) benzoic acid showed highest docking score of -5.8214, which is important for HDAC8 inhibition. In this present investigation, molecular docking, design, synthesize and evaluated for *in vitro* antitumor activity to identify novel active compound targeting the HDAC8 protein. Among the 19 compounds A19 showed promising activity against human cervical cancer cell line.

INTRODUCTION:

Cancer is a generic term for a group of over 100 chronic diseases, which can affect any part of the body .For a number of years now, a number of potential approaches have been proposed for the treatment of cancer. One of the recent targets is Histone Deacetylase (HDAC). The members of the classical HDAC family fall into two different phylogenetic classes, namely class I and class II. Deacetylation is a process that removes acetyl group from the Histone tails, causing the Histone to wrap more tightly around the DNA and interfering with the transcription of genes by blocking access by transcription factors. The overall result of Deacetylation is a non-specific reduction in the gene expression.

The tumor-suppressor gene RB requires the recruitment of class I HDACs to repress gene transcription Thus, the loss of class I HDAC activity could induce the expression of genes regulated by Rb, thereby suppressing their protective role in tumour development. Histone deacetylase is one of the main targets for cancer disease. Chromatin structure of histone has two forms as Histone acetylases and Histone deacetylases[1] HDACs are involved in cell-cycle progression and differentiation, and their deregulation is associated with several cancers[2]. Development of HDAC inhibitors as anti cancer drugs has been initiated recently. The present investigation involves molecular docking studies of virtually designed naphthylidene base of benzoic acid derivatives and the synthesis and evaluation of *in vitro* anti tumour activity potential HDAC8 inhibitors.

MATERIALS AND METHODS:

Computational Design to choose best novel heterocyclic compound derivatives based on target based drug discovery:

Total 19 compounds are designed virtually based on the QSAR and pharmacophore model[3] as 4-{(E)-[(2-Hydroxy-1-naphthyl)methylene]amino}benzoic acid (Fig. 1). Naphthylidene base of Benzoic acid derivative is optimized using aromatic and acceptor groups and the ligands are listed in Table 1. The ligands are sketched using ISIS Draw and these are given as input to prepare ligand module in Glide. This generates 3D structures, tautomers, isomers and filters the ligands by Lipinski rule of five. After applying the force fields on ligands the structures are minimized for lowest energy.
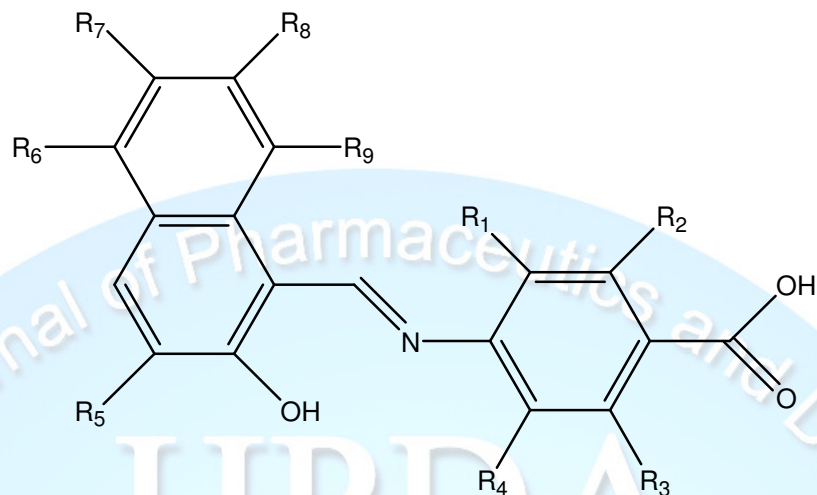
Jebastin JNS et al, *Int J. Pharm. Drug. Anal*, Vol: 3, Issue: 12, 2015; 385-393

Available online at http://ijpda.com

.

Figure 1: Parent nucleus of naphthylidene base of benzoic acid derivative

Table 1: Naphthylidene base of Benzoic acid derivatives (A1-A19)

Compound	R1	R2	R3	R4	R5	R6	R7	R8	R9
A1	H	H	H	H	OH	H	OH	H	H
A2	H	H	H	H	OH	H	OH	H	CH₃
A3	H	H	H	H	OH	CH₃	OH	H	CH₃
A4	H	H	H	H	OH	CH₃	OH	OH	CH₃
A5	H	CH₃	H	H	OH	CH₃	OH	OH	CH₃
A6	H	CH₃	CH₃	H	OH	CH₃	OH	OH	CH₃
A7	H	OH	OH	H	OH	CH₃	OH	OH	CH₃
A8	CH₃	OH	OH	H	OH	CH₃	OH	OH	CH₃
A9	CH₃	OH	OH	H	OH	CH₃	OH	OH	CH₃
A10	CH₃	OH	OH	OH	OH	CH₃	OH	OH	CH₃
A11	OH	OH	OH	OH	OH	CH₃	OH	OH	CH₃
A12	OH	OH	OH	OH	OH	CH₃	OH	OH	OH
A13	OH	Cl	OH	OH	OH	CH₃	OH	OH	OH
A14	OH	Cl	Cl	OH	OH	CH₃	OH	OH	OH
A15	OH	Cl	Cl	OH	CH₂CH₃	CH₃	OH	OH	OH
A16	OH	H	H	OH	CH₂CH₃	CH₃	OH	OH	OH
A17	OH	H	H	OH	CH₂CH₃	H	OH	H	H
A18	H	H	H	H	H	H	OH	H	H
A19	**H**	**H**	**H**	**H**	**H**	**H**	**H**	**H**	**H**

Docking Methodology:

The steps involved in docking are as follows:

Ligand structure: The chemical structure of each ligand was drawn using build module.

Ligand preparation: In order to prepare high quality, all-atom 3D structures for large numbers of drug-like molecules, starting with the 3D structures in SD Maestro format, LigPrep was used. LigPrep produced a single, low energy and 3D structure for each successfully processed input structure.

Preparation of protein: Molecular docking were performed for 19 compounds using the GLIDE program (Version 5.0, Schrodinger, LLC, New York, 2008) to understand the interaction of 3k with HDAC8. The Maestro user interface (version8.5, Schrodinger, LLC, New York, 2008) was employed to set up and execute the docking protocol and also for analysis of the docking results. Human HDAC8 (PDB ID: 1T69) was selected for docking studies and was prepared for docking through protein preparation wi-

zard, energy minimization has been carried out using OPLS2001 force field. Maestro and prepared for docking through Ligprep module (energy minimized using MMFF force field). GLIDE grid generation wizard has been used to define the docking space. Docking was performed using SP (Standard Precision mode) docking protocol.

Receptor Grid Generation: Receptor grid generation requires a "prepared" structure: an all atom structure with appropriate bond orders and formal charges. Glide searches for favourable interactions between one or more ligand molecules and a receptor molecule, usually a protein. The shape and properties of the receptor are represented on a grid by several different sets of fields that provide progressively more accurate scoring of the ligand poses. The options in each tab of the Receptor Grid Generation panel allow defining the receptor structure by excluding any co-crystallized ligand that may be present, determine the position and size of the active site as it will be represented by receptor grids, and set up Glide constraints. A grid area was generated around the binding site of the receptor.

Ligand Docking: This is carried out using Glide Dock. Glide searches for favourable interactions between one or more ligand molecules and a receptor molecule, usually a protein. Each ligand acts as single molecule, while the receptor may include more than one molecule, e.g., a protein and a cofactor. Glide was run in rigid or flexible docking modes; the latter automatically generated conformations for each input ligand. The combination of position and orientation of a ligand relative to the receptor, along with its conformation in flexible docking, is referred to as a ligand pose. The ligand poses that Glide generates pass through a series of hierarchical filters that evaluate the ligand's interaction with the receptor. The initial filters test the spatial fit of the ligand to the defined active site, and examine the complementarity of ligand-receptor interactions using a grid-based method patterned after the empirical ChemScore function. Poses that passed these initial screens entered the final stage of the algorithm, which involves evaluation and minimization of a grid approximation to the OPLS-AA non bonded ligand-receptor interaction energy. Final scoring is then carried out on the energy-minimized poses.

Glide Extra-Precision Mode (XP): The extra-precision (XP) mode of Glide combines a powerful sampling protocol with the use of a custom scoring function designed to identify ligand poses that would be expected to have unfavourable energies, based on a well-known principles of physical chemistry. The presumption is that only active compounds will have available poses that avoid these penalties and also receive favourable scores for appropri-

ate hydrophobic contact between the protein and the ligand, hydrogen-bonding interactions, and so on. The chief purposes of the XP method are to weed out false positives and to provide a better correlation between good poses and good scores. Extra-precision mode is a refinement tool designed for use only on good ligand poses. Finally, the minimized poses are re-scored using Schrödinger's proprietary GlideScore scoring function. GlideScore is based on ChemScore, but includes a steric-clash term and adds buried polar terms devised by Schrodinger to penalize electrostatic mismatches: Glide Score = 0.065*vdW + 0.130*Coul + Lipo + Hbond + Metal + BuryP + RotB + Site.

QikProp[4] is a quick, accurate, easy-to-use absorption, distribution, metabolism, and excretion (ADME) prediction program designed by Professor William L. Jorgensen. QikProp predicts physically significant descriptors and pharmaceutically relevant properties of organic molecules, either individually or in batches. In addition to predicting molecular properties, QikProp provides ranges for comparing a particular molecule's properties with those of 95% of known drugs. QikProp also flags 30 types of reactive functional groups that may cause false positives in high-throughput screening (HTS) assay.

Synthesis:
Synthesis of 4-((2-hydroxynaphthalen-1-yl) methyleneamino)benzoic acid :
Exactly 1.72g (10mmol) of 2-Hydroxynaphthaldehyde was dissolved in 50ml of methanol and taken in a 150ml beaker. Exactly 1.37g (10mmol) of 4-Amino benzoic acid was dissolved separately in 50ml of methanol. The methanolic solution of 2-Hydroxynaphthaldehyde was stirred vigorously at room temperature using a magnetic stirrer. Then the methanolic solution of 4-Aminobenzoic acid was added in drops to the above solution with constant stirring for a period of 20 minutes. Yellow precipitate was formed after the complete addition of the amine solution. To ensure the completion of the reaction, the reaction mixture was further stirred for another 6h at room temperature. After 6h of stirring at room temperature, the reaction mixture was refluxed at 60^0 C for half an hour with constant stirring. Then the reaction mixture was cooled to room temperature. The yellow precipitate formed was filtered, washed several times with cold methanol and dried over calcium chloride in a desiccator. The Schiff base 4-((2-hydroxynaphthalen-1-yl)methyleneamino) benzoic acid A19 was obtained as an yellow solid in 84% (2.434g) yield.

Characterization
FTIR Analysis:
IR spectra of all Schiff bases and their metal complexes were obtained in Perkin Elmer FTIR spectrometer using

Potassium Bromide pellets in the range of 400-4000 cm^{-1}

NMR Studies:

^{1}H-NMR experiments for all the Schiff bases synthesized were performed in a BRUKER 500 MHz NMR instrument. About 2-3mg of ligands was dissolved in 0.5ml of CDCl$_3$ in a NMR tube. About 50 scans were performed for every spectrum. In all the cases Tetramethylsilane (TMS) was used as an internal standard. All the spectra obtained were corrected with respect to TMS. The software Mestrec 2.0 was used to evaluate the peak positions and their integrations.

^{13}C-NMR experiments for all the Schiff bases synthesized were performed in a Bruker 125 MHz NMR instrument. About 30-40mg of ligands was dissolved in 0.5ml of either DMSO-d$_6$ or CDCl$_3$ in a NMR tube. About 1000 scans were performed for all the experiments. All the spectra obtained were corrected with respect to the solvent signal.

UV-VIS Spectroscopy:

The UV-Vis spectra for all the Schiff bases and their metal complexes were obtained in 10^{-3} M solution of Ethanol at room temperature using Perkin Elmer UV-Vis-NIR spectrometer. Glass cuvettes were used for the measurements in the UV-Vis region. The baseline was corrected with respect to ethanol in all the case. For all experiments the spectral range was scanned from 200-800nm. The scan rate was kept constant (100nm/sec) for all the experiments.

Fluorescence Spectroscopy:

The fluorescence spectra for all the Schiff bases and their metal complexes were performed in a10^{-6} M solution of ethanol at room temperature using a Perkin Elmer LS-55 spectrofluorometer. Quartz fluorescence cell were used for the measurements in the solution state. The excitation and emission slit width was maintained at 5.0nm for all the experiments. The sample was either excited at 270nm or at 380nm. The fluorescence spectra were recorded over the range 200-800nm. A slow scan rate was maintained for all the experiments.

Mass Spectroscopy:

The GC-MS spectra of the compounds were recorded on Varian Saturn 2200 GC/MS/MS spectrophotometer using electron impact method where the electronic accelerating voltage is 75 eV and the ion accelerating voltage is 8 – 10 kV.

In Vitro Anti Cancer Activity[5]:

The human cervical cancer cell line (HeLa) was obtained from National Centre for Cell Science (NCCS), Pune, and grown in Eagles Minimum Essential Medium containing 10% fetal bovine serum (FBS).

For screening experiment, the cells were seeded into 96-well plates at plating density of 10,000 cells/well and incubated to allow for cell attachment at 37^{0}C, 5% CO$_2$, 95% air and 100% relative humidity[6-8]. After 24h the cells were treated with serial concentrations of the samples. The samples were initially dissolved in dimethylsulphoxide (DMSO) and further diluted in serum free medium to produce five concentrations. One hundred microliters per well of each concentration was added to plates to obtain final concentrations of 100, 10, 1, 0.1μM. The final volume in each well was 200μl and the plates were incubated at 37^{0}C, 5% CO$_2$, 95% air and 100% relative humidity for 48h. The medium containing without samples were served as control. Triplicate was maintained for all concentrations[9-10].

After 48h of incubation, 15μl of MTT (5mg/ml) in phosphate buffered saline (PBS) was added to each well and incubated at 37^{0}C for 4h. The medium with MTT was then flicked off and the formed Formosan crystals were solubilized in 100μl of DMSO and then measured the absorbance at 570nm using micro plate reader. The % cell inhibition was determined using the following formula[11].

% cell Inhibition = 100- Abs (sample)/Abs (control) x100

Nonlinear regression graph was plotted between % Cell inhibition and Log$_{10}$ concentration and IC$_{50}$ was determined using Graph Pad Prism software

RESULTS AND DISCUSSION

All the 19 ligands were docked in the active site of Human HDAC8 (PDB ID: 1T69) using Glide Dock. Compounds were ranked based on the docking score. The docking score of all ligands are presented in Table 2. Heterocyclic functional group of all the molecules were found to be close to Zn^{2+} atom in the active site, and establishes a hydrogen bond with (A19) ASP331, which shows the major and favourable interaction of the ligands with HDAC8. Among the 19 molecules docked, compound A19 was the one with the best Glide and E model score of (-41.4789) (Fig. 2). It exhibited one hydrogen bonding interaction with active site amino acids.

Table 2: Components of Glide Score of Docking (Extra-Precision Mode)

Code	XP GScore	glide e model	glide energy	XP HBond	glide pose no.
A19	-5.8214	-41.4789	-31.4478	-0.90	3

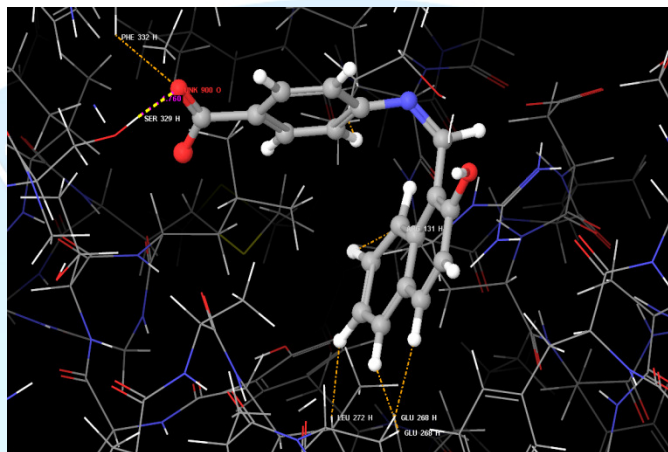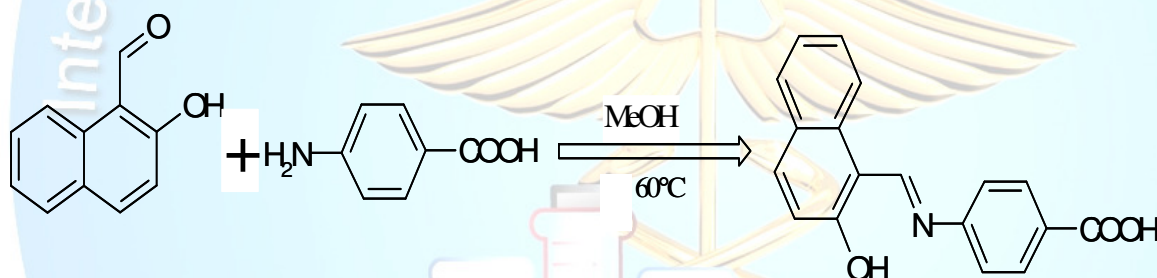**Figure 2: HDAC8 molecular interaction with compound A19**

Scheme 1: Synthesis of 4-((2-hydroxynaphthalen-1-yl) methyleneamino) benzoic acid

Jebastin JNS et al, *Int J. Pharm. Drug. Anal*, Vol: 3, Issue: 12, 2015; 385-393
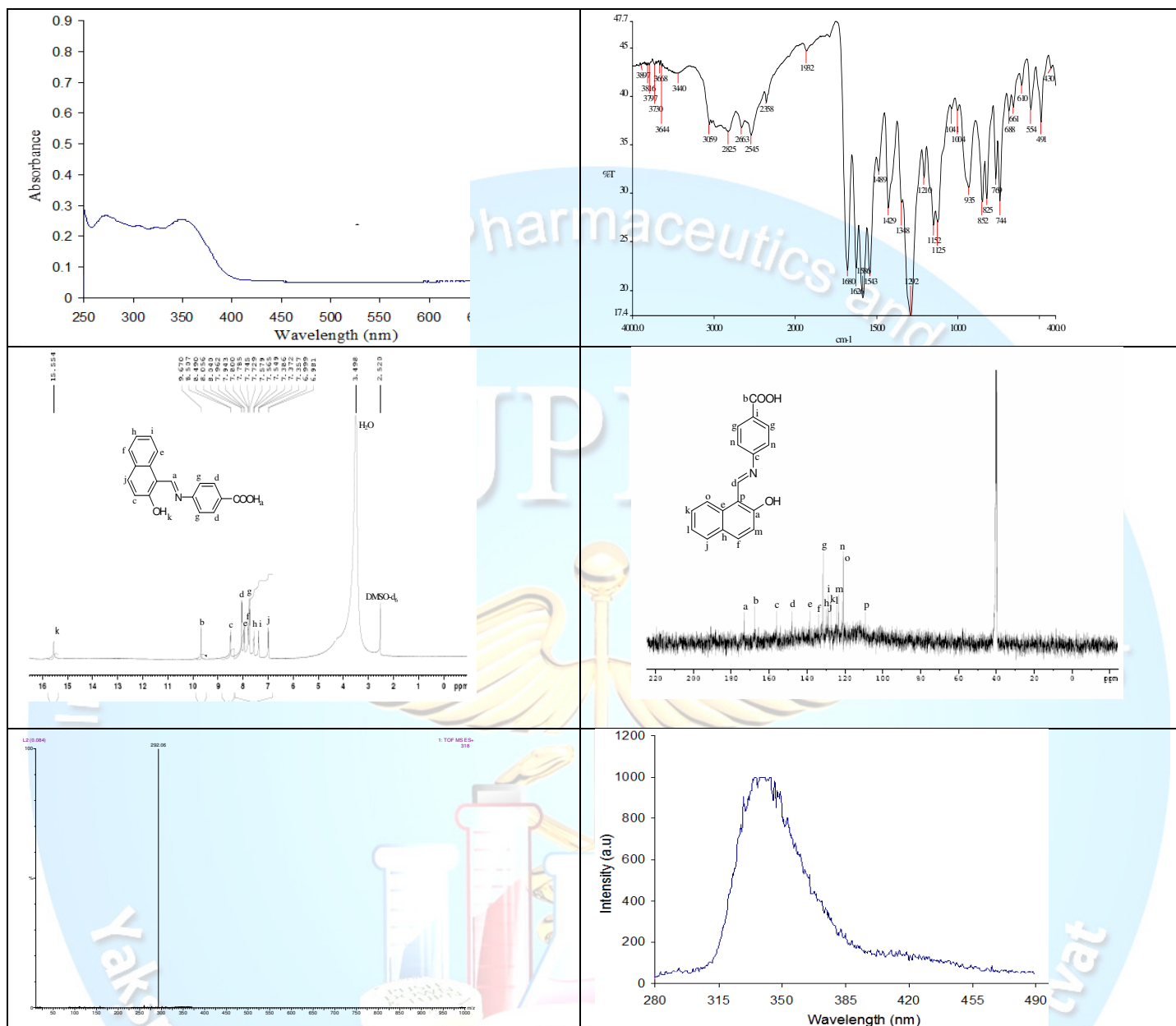
Available online at http://ijpda.com

Figure 3: Spectral studies of compound A19 (a): UV-Vis spectra of ligand A19 in ethanol at 25°C; (b): FTIR spectrum of Schiff base; (c): ¹H-NMR spectra in CDCl₃; (d): ¹³C-NMR (¹H decoupled) spectra in CDCl₃; (e): Mass Spectrum; (f): Fluorescence spectra in ethanol at 25°C (λex = 270nm).

Synthesis:

The synthetic route for compound A19 shown in scheme 1. The methanolic solution of 2-Hydroxy naphthaldehyde was stirred with the methanolic solution of 4-amino benzoic acid vigorously at room temperature produced 4-((2-hydroxynaphthalen-1-yl) methyleneamino) benzoic acid as yellow precipitate.

UV-VIS Spectrum:

The UV-Vis spectrum of the compound A19 is recorded in 10^{-6} M solution of ethanol at room temperature. Figure 3(a) depicts the UV-Vis spectra of A19. Two broad bands

at 270 and 355nm are observed in the UV-Vis spectra of A19. The band at the 270nm is attributed to the benzene π-π* transition. Another band at 355nm is due to n- π* transition of the non-bonding electrons present on the nitrogen of the azomethine group in Schiff base.

IR spectrum:

The IR spectrum of Schiff base compound A19 is given in Figure 3(b). The characteristic band at 1586cm⁻¹ corresponds to the presence of –C=N group in the molecule which in turn suggest the formation of Schiff base. A strong and intense band is also observed in 1680cm⁻¹ cor-

390

Jebastin JNS et al, *Int J. Pharm. Drug. Anal*, Vol: 3, Issue: 12, 2015; 385-393

Available online at http://ijpda.com

responds to the –C=O stretching frequency of carbonyl unit in the molecule. The Schiff base also showed a broad intense band peak 3440cm^{-1}, a characteristic feature for –OH and –COOH groups stretching frequency indicating the existence of free –OH group and –COOH groups in the Schiff base.

¹H-NMR studies:
The ¹H NMR Spectra of ligand compound A19 is shown in the Figure 3(c). The spectra of ligand A19 consists of 5 sets of non equivalent proton. The signal at δ=15.5ppm is due to the proton of phenolic group. The signal at δ=9.6ppm is due to the proton of azomethine group (CH=N-).The signal at δ=8.6-6.9 is due to protons of the aromatic rings. It supports the overall structure of the product and conform the product formation.

¹³C-NMR Studies:
The ¹³C-NMR spectrum of compound A19 is shown in Figure 3(d). The spectrum of compound A19 consists of many sets of non equivalent carbon atoms. The Peak observed at 171and 169ppm are due to cabonyl carbon and C-O carbon phenyl ring. These carbon atoms are highly deshielded, because it is a part of the carbonyl group and hence the signal appears at downfield. The peak at 158 and 153ppm are due to C-N and azomethine carbon. The regions from 133-108ppm are assigned to aromatic carbons, which has high intense signals. But the quaternary carbon shows the lower intensity signal.

Mass Spectra:
The mass spectrum of A19 recorded in Ethanol and depicted in Figure 3(e). It indicating a intense molecular ion peak at δ292.6 correspond to respective (M+H)[+] molecular formulae, confirms the formation of compound A19.

Fluorescence spectrum:
The fluorescence emission spectra of compound A19 is recorded in 10^{-6} M solution of Ethanol at room tempera-

ture. Figure 3(f) depicts the fluorescence emission spectra of compound A19. An emission band was observed in the region of 320-385nm on excitation at 270nm. This may be attributed to the monomer emission of the naphthalene molecules in the ligand. A broad band in the longer wavelength region (390-450nm) is also observed which can be assigned as either excimer/exciplex emission. The molecules in solution state can self-assemble in such a fashion to a form π-π stacking between either two units of naphthalene or one of naphthalene or the other unit of phenyl moiety.

In Vitro Anti Cancer Activity:
The anti tumour activity of compounds against human cervical cancer cell line (SiHa) was determined by MTT assay method. The human cervical cancer cell line (SiHa) was obtained from National Centre for Cell Science (NCCS), Pune, and grown in Eagles Minimum Essential Medium containing 10% fetal bovine serum (FBS). Cell line was incubated with different concentration for compound A19 and was used to create concentration in various percentage of cell inhibition. These response parameter (IC₅₀) was calculated for each cell line. The synthesized pyrazole derivative compounds were screened against screened (HeLa) human cervical cancer cell line at different concentration are shown in Table 3 and Figure 4.

The IC₅₀value corresponds to the compound concentration causing a net 50% loss of initial cells at cell of the incubation period. Compound A19 was found to be more potent and it shows the IC₅₀ value at 17.84μM. The standard drug 5-fluro uracil IC₅₀ value at 2.836μM revealing that the potency of compound A19 was closer to that of the standard drug IC₅₀ value. The higher anticancer potency of compound A19 is probably due to the presence benzene moiety in the 4-aminoantipyrine. This might be the reason for the notable difference in IC₅₀ values of the synthesized heterocyclic derivatives.

Table 3: The synthesized benzoic acid derivative compounds were screened against screened (HeLa) human cervical cancer cell line at different concentration

Code	Cell line	Concentration (μM)	% cell inhibition
Compound A19	HeLa	0.1	3.627968
		1	12.26913
		10	32.38786
		100	54.8153
STD (5-fluro Uracil)	HeLa	0.1	6.675567
		1	30.70761
		10	71.49533
		100	99.3992

Jebastin JNS et al, *Int J. Pharm. Drug. Anal*, Vol: 3, Issue: 12, 2015; 385-393
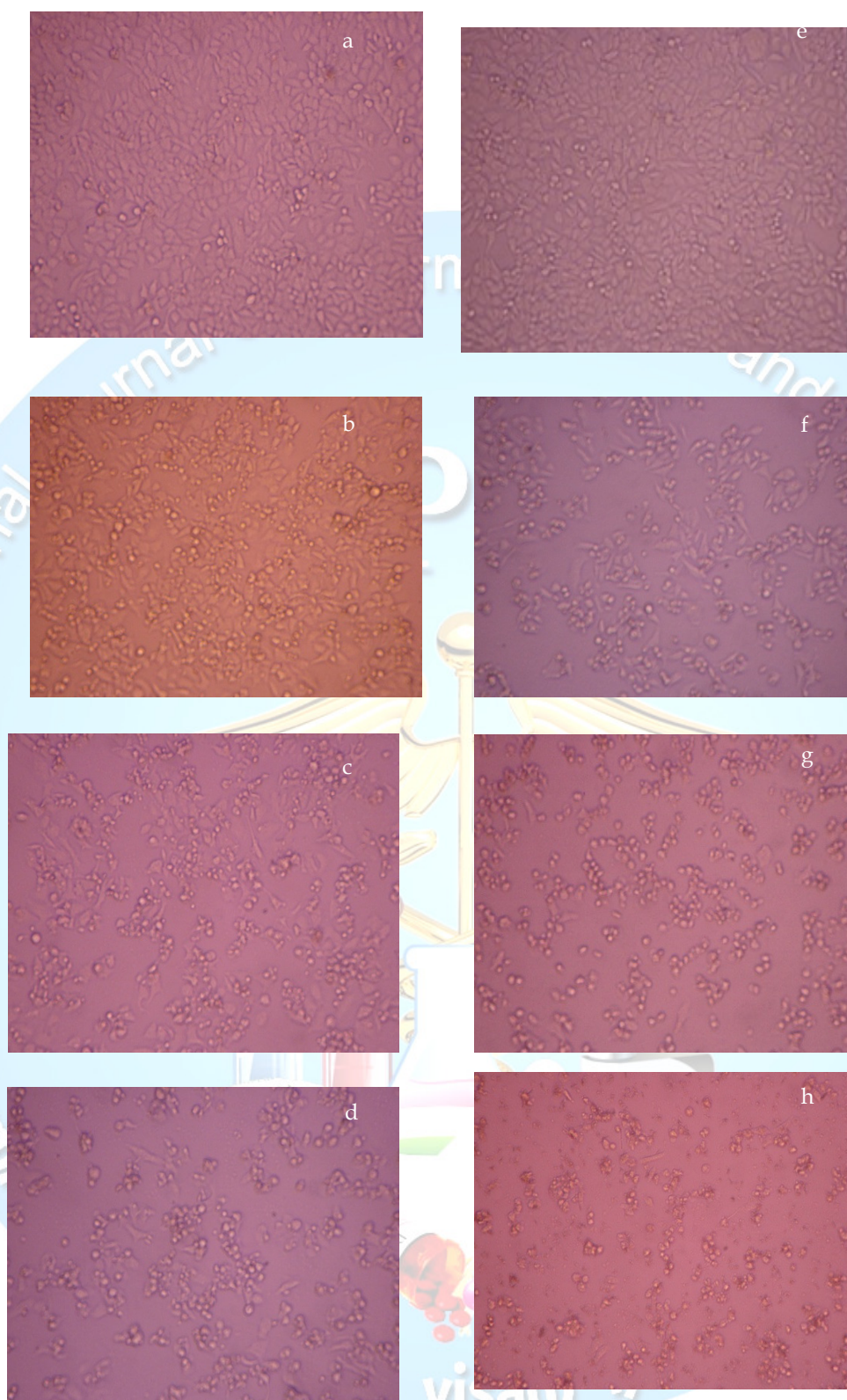
Available online at http://ijpda.com

Figure 4:HeLa cell line inhibition by the sample compound (a,b,c,d) and standard drug (5-fluoro uracil) (e,f,g,h) at 0.1, 1 10 and 100μM

Jebastin JNS et al, *Int J. Pharm. Drug. Anal*, Vol: 3, Issue: 12, 2015; 385-393

Available online at http://ijpda.com

REFERENCES

1. Monneret C., Histone deacetylase inhibitors. Eur J Med Chem, 40: 1–13, 2005.

2. Kouzarides T., Histone acetylases and deacetylases in cell proliferation. Curr Opin Genet Dev. 9: 40-8, 1999.

3. Naresh K., Geetha Ramakrishnan V., Sarma Jagarlapudi S., QSAR Studies of N-(2-Aminophenyl)- Benzamide derivatives as Histone deacetylase2 Inhibitors. Int J PharmTech Res. 4: 1110-1121, 2012.

4. Ioakimidis L., Loizos T., Amin M., Saira N., Johannes R., Benchmarking the reliability of QikProp. Correlation between experimental and predicted values. QSAR & Comb Sci. 27(4): 445-456, 2008.

5. Wang W., Yuqing Z., Elizabeth RR., Donald LH., Hui W., Ruiwen Z., *In vitro* anti-cancer activity and structure–activity relationships of natural products isolated from fruits of Panax ginseng. Cancer Chemother Pharmacol. 59(5): 589-601, 2007.

6. Boyd MR., Paull KD., Some practical considerations and applications of the National Cancer Institute *in vitro* anticancer drug discovery screen. Drug Dev. Res. 34: 91-109, 1995.

7. Tamm I., Yan Wang ED., Sausville DA., Scudiero NV., Tilman O., John CR., IAP-family protein survivin inhibits caspase activity and apoptosis induced by Fas (CD95), Bax, caspases, and anticancer drugs. Cancer Res. 58(23): 5315-5320, 1998.

8. Johnson JI., Decker S., Zaharevitz D., Rubinstein LV., Venditti JM., Schepartz S., Kalyandrug S., Christian M., Arbuck S., Hollingshead M., Sausville EA., Relationships between drug activity in NCI preclinical *in vitro* and *in vivo* models and early clinical trials. Br J Cancer. 84(10): 1424, 2001.

9. Shoemaker M., Bobbi Hamilton SH., Dairkee IC., Michael JC., *In vitro* anticancer activity of twelve Chinese medicinal herbs. Phytotherapy Res. 19(7): 649-651, 2005.

10. Kelter G., Nigel JS., Katja S., Heinz Herbert F., Matthias T., *In-vitro* anti-tumor activity studies of bridged and unbridged benzyl-substituted titanocenes. Anti-Cancer Drugs. 16(10): 1091-1098, 2005.

11. Seeram NP., Lynn SA., Susanne MH., Yantao N., Yanjun Z., Muraleedharan GN., David H., *In vitro* antiproliferative, apoptotic and antioxidant activities of punicalagin, ellagic acid and a total pomegranate tannin extract are enhanced in combination with other polyphenols as found in pomegranate juice. J Nutr Biochem. 16(6): 360-367, 2005.